

See discussions, stats, and author profiles for this publication at: <https://www.researchgate.net/publication/237839444>

Generation of Antibubbles from Core-Shell Double Emulsion Templates Produced by Microfluidics

ARTICLE *in* LANGMUIR · JUNE 2013

Impact Factor: 4.46 · DOI: 10.1021/la4009015 · Source: PubMed

CITATIONS

5

READS

17

4 AUTHORS, INCLUDING:



Justin Silpe

Princeton University

10 PUBLICATIONS 170 CITATIONS

SEE PROFILE



Albert T. Poortinga

Technische Universiteit Eindhoven

26 PUBLICATIONS 587 CITATIONS

SEE PROFILE

Generation of Antibubbles from Core–Shell Double Emulsion Templates Produced by Microfluidics

Justin E. Silpe,^{†,‡} Janine K. Nunes,[‡] Albert T. Poortinga,[§] and Howard A. Stone^{‡,*}

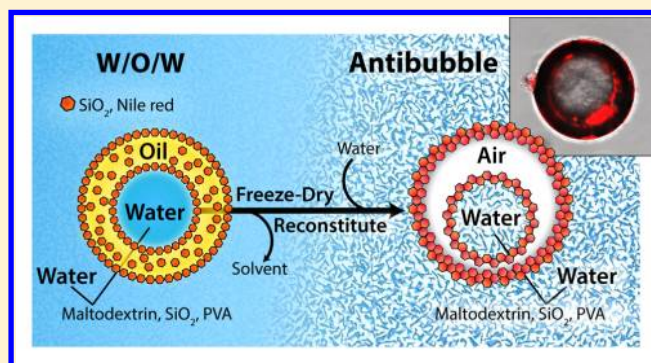
[†]Department of Macromolecular Science and Engineering, University of Michigan, Ann Arbor, Michigan 48109, United States

[‡]Department of Mechanical and Aerospace Engineering, Princeton University, Princeton, New Jersey 08544, United States

[§]FrieslandCampina Research, Harderwijkerstraat 6, 7418 BA Deventer, The Netherlands

S Supporting Information

ABSTRACT: We report the preparation of antibubbles by microfluidic methods. More specifically, we demonstrate a two-step approach, wherein a monodisperse water-in-oil-in-water (W/O/W) emulsion of core–shell construction is first generated via microfluidics and freeze-dried thereafter to yield, upon subsequent reconstitution, an aqueous dispersion of antibubbles. Stable antibubbles are attained by stabilization of the air–water interfaces through a combination of adsorbed particles and polymeric surfactant. The antibubbles strongly resemble the double emulsion templates from which they were formed. When triggered to release, antibubbles show complete release of their cores within about 100 ms.



1. INTRODUCTION

Antibubbles are liquid droplets encaged by a shell of gas within a continuous liquid phase. Such structured materials have several promising applications, for example, as controlled release systems and as building blocks of nondraining foams. A major hurdle in the implementation of antibubbles has been their inherent instability, leading to lifetimes of at most minutes if not actually much more ephemeral existences.^{1,2} Recently, methods have been proposed to produce antibubbles in the micrometer size range³ and with long-term stability.⁴ In this approach, the antibubbles derive their stability from the interfacial adsorption of colloidal particles; that is, so-called Pickering stabilization was applied.^{5,6} Specifically, antibubbles were obtained by first making a water-in-oil-in-water (W/O/W) emulsion in which the aqueous phases contain a glass-forming solute and the oil is volatile. Subsequent removal of the volatile oil (and residual water) through freeze-drying and redispersion of the resulting powder produced antibubbles.

Until now, antibubbles have been made from W/O/W emulsions produced by classical high-shear emulsification methods, and as a result, the properties of the antibubbles, such as their overall size and the thickness of their gas shell, have been difficult to manipulate. Although the production of stable antibubbles in the micrometer range constitutes an important step toward potential applications, the poor control over their properties is a significant limitation. For example, antibubbles can be used for triggered release only under well-defined conditions when their shell thickness can be controlled. Similarly, in order to make a nondraining foam composed of antibubbles, the density of the constituents must precisely reflect that of the continuous phase.

In light of the inherent limitations of conventional, two-step emulsification, we employ droplet-based microfluidics using consecutive flow-focusing (CFF) geometries to generate monodisperse W/O/W emulsions stabilized by colloidal silica (SiO_2) and poly(vinyl alcohol) (PVA). The monodisperse W/O/W emulsions are freeze-dried to remove all solvent and then reconstituted in water to produce antibubbles, as described schematically in Figure 1. The resulting antibubbles are subject to significantly greater control, over both size and content, than what was otherwise possible through prior approaches.

2. EXPERIMENTAL SECTION

Unless otherwise stated, all chemicals were purchased from Sigma–Aldrich and were used as received.

2.1. Device Fabrication. Microfluidic devices were fabricated from a commercially available Dow Corning Sylgard 184 poly-(dimethylsiloxane) (PDMS) kit (Ellsworth Adhesives) by standard soft lithography techniques.⁷ Briefly, the kit, containing both precursor and cross-linker, was mixed at the recommended 10:1 (w/w) ratio and transferred to a silicon wafer containing the positive relief of the CFF microchannel pattern. The mixture was cured at 65 °C for 2 h, after which individual devices were cut out from the PDMS cast and detached from the wafer. Inlets and outlets were made with a 1 mm biopsy punch. The microfluidic devices were then assembled by uniting the PDMS cast with a glass slide. A strong bond was achieved by use of a hand-held Corona surface treater (Electro-Technic Products, Inc.), which was applied to each surface for 20–30 s immediately prior to assembly.

Received: March 11, 2013

Revised: May 17, 2013

Published: June 12, 2013

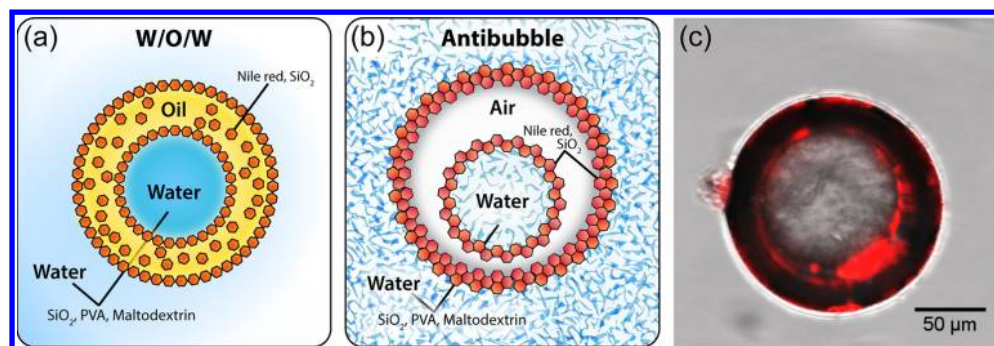


Figure 1. Schematic representation of the structure and stepwise production of antibubbles templated from W/O/W double emulsions. (a) Core-shell W/O/W template, as produced by microfluidics. (b) Antibubble structure, generated after freeze-drying and reconstituting the template. An antibubble is produced when the middle phase oil is replaced with air, resulting in its unique core-hollow shell construction. The apparent texture at the inner and outer regions denotes a glassy maltodextrin matrix which forms in the aqueous phases as a result of freeze-drying. (c) Confocal composite of an antibubble produced as described. The interfaces light up red due to the presence of the fluorescent dye, Nile red.

2.2. Surface Preparation. In order for a stable emulsion to form, the microchannel surface must be tailored to the wettability of the continuous phase.⁸ Thus, in the case of our W/O/W double emulsions, produced by a two-step droplet breakup process, the surface must be modified locally to accommodate a W/O emulsion at the first junction and a W/O/W emulsion at the second junction. Accordingly, selective wettability in the current microfluidic devices was achieved by photoinduced graft polymerization of acrylic acid, as described by Schneider et al.⁸ Briefly, a microfluidic device was first primed with a 12 wt % solution of benzophenone photoinitiator dissolved in acetone and vacuum-dried for 10 min. A degassed monomer solution, consisting of 12–15 wt % acrylic acid in deionized (DI) water, was then loaded into the primed microfluidic device and temporarily sealed with translucent adhesive tape. Patterning was achieved by carefully positioning a piece of black electrical tape over and about the segment between the first and second flow-focusing junctions to effectively inhibit photopolymerization in that region. The device was then placed upside down (glass side up) in a UV flood curing system (Intelli-Ray 400 shuttered UV floodlight, Uvitron International) for photopolymerization. A 365–610 nm band-pass filter was stacked on top of the device to avoid monomer evaporation within the device and a correspondingly inconsistent polymerization. UV exposure was carried out for 200–400 s at an effective intensity of approximately 45 mW/cm². After exposure, excess monomer solution was flushed out of the system and washed with ethanol and DI water at pH 10 prior to subsequent use.⁸

2.3. Double Emulsion Preparation. Three fluid phases were used in the fabrication of W/O/W double emulsions (Figure 2). The inner and outer aqueous phases were composed of 25 and 5 wt % maltodextrin 33DE (supplied by Roquette) and 0.2 and 2.0 wt % PVA (M_w 85 000–124 000), respectively, in DI water. The outer aqueous phase also contained 2.0 wt % Aerosil R816 hydrophobic silica (12 nm average primary particle size; supplied by Evonik), not present in the inner aqueous phase, and was supplemented with potassium hydroxide to obtain an outer phase pH = 10. The middle phase fluid was composed of 3.0 wt % HDK H18 hydrophobic silica (5–30 nm primary particle size; supplied by Wacker) in decane, with 0.2 wt % Nile red added for imaging by confocal laser scanning microscopy (CLSM, Leica SP5) and fluorescence microscopy (Leica DMI4000B). Hydrophobicity was quantified in terms of relative carbon content, which ranges from 4.5 wt % in HDK H18 (more hydrophobic) to 0.9–1.8 wt % in R816 (less hydrophobic). The use of less hydrophobic particles in the outer aqueous phase is analogous to the situation of surfactant-stabilized W/O/W double emulsions where one typically reserves the most hydrophobic surfactant for the innermost interface, as shown by Barthel et al.⁹ Furthermore, a pH of 10 was selected for the outer phase in order to give the adsorbed R816 particles a more negative charge at the interface,¹⁰ so as to promote better stabilization of the W/O/W droplets against coalescence. Each phase was loaded into a syringe and secured to its respective inlet on the PDMS device

with polyethylene tubing. Syringe pumps (Harvard Apparatus and New Era Pump Systems) were used to dispense each phase at a prescribed flow rate for the duration of the experiments. For the production of the current W/O/W emulsions, typical flow rates for the inner, middle, and outer phases were 1.2, 3, and 10 μ L/min respectively.

3. RESULTS AND DISCUSSION

Monodisperse (W/O/W) double emulsions were generated by use of a PDMS microfluidic device with consecutive flow-focusing geometries as shown in Figure 2. Stable double emulsions were formed only when PVA was added to the aqueous phases in addition to the silica particles. This result is in line with the work of Sander et al.,¹¹ who showed that PVA and hydrophobized silica together form a strong elastic film at the interface through the “cross-linking” of silica particles by the PVA. The observation that particles alone do not stabilize microfluidically generated double emulsions is likely due to insufficient particle adsorption at the low Reynolds numbers prevailing in microfluidic systems.¹²

3.1. Freeze-Drying. W/O/W emulsions were collected upon production in 2 mL vials and placed in a low-temperature chest freezer (Dairei SUF 100) at -79 $^{\circ}$ C, to be lyophilized soon thereafter. Lyophilization or freeze-drying, as applied to our double emulsion templates, involves a three-step process in which the solvent among all three phases (inner, middle and outer) is first crystallized, by cooling the sample at some subfreezing temperature, and then dried in vacuo to remove the frozen solvent from the remaining material.¹³ This was achieved by placing a collection vial of frozen sample into a freeze-drying flask and attaching it to the vacuum manifold of a freeze-dryer (VirTis Benchtop). Lyophilization was performed at -77 $^{\circ}$ C under reduced pressure (200 mTorr) for a period of 20–30 h.

The oligosaccharide maltodextrin, which does not crystallize upon freeze-drying, was used to promote the formation of an amorphous glassy matrix in both the core and continuous phases. As residual ice is removed by sublimation, the amorphous matrix is retained in the glassy state. This feature of processing allows for both a porous and robust core and continuous phase and ensures that evolution of oil from the middle phase does not result in completely hollow or conversely collapsed structures in the final product. Furthermore, maltodextrin is expected to give a more robust glass than smaller saccharides because of its relatively high special glass transition temperature (T_g'). Accordingly, removal of the organic (middle phase) solvent is confined to the space

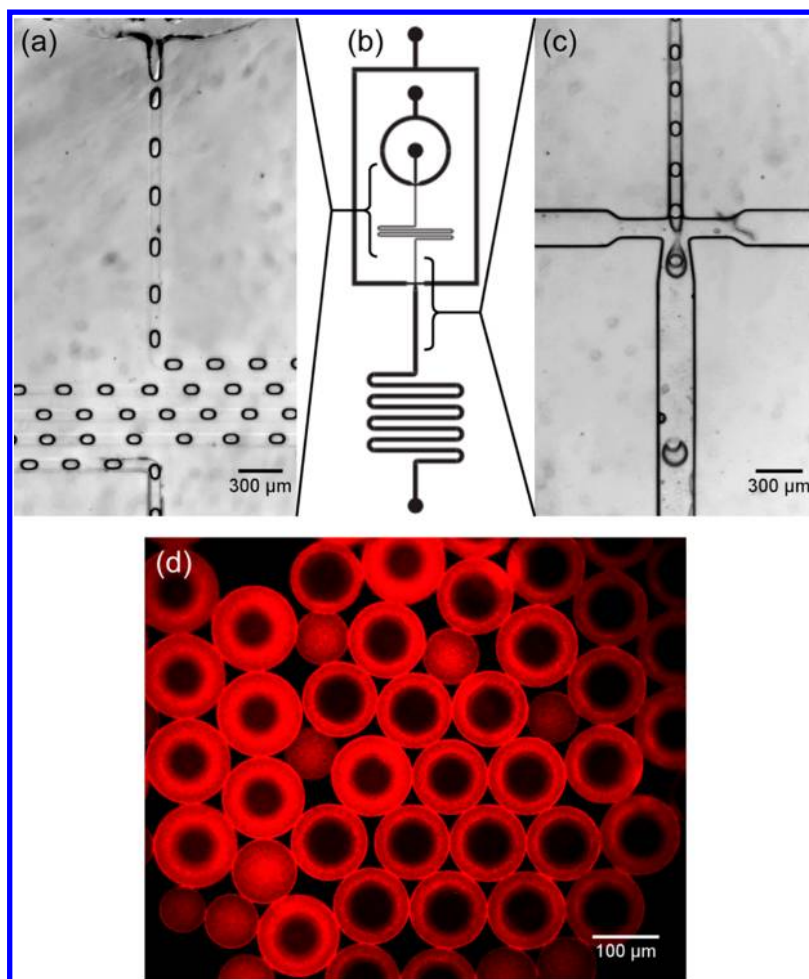


Figure 2. Generation of W/O/W emulsions in a consecutive flow-focusing device. (a) Optical micrograph of W/O formation at the first flow-focusing junction. (b) Schematic layout of the device used to produce W/O/W emulsions. The inner and outer aqueous phases were injected into the third and first inlets (from the top), while the middle decane phase is injected through the second inlet. (c) Optical micrograph of W/O/W droplet formation at the second of two flow-focusing junctions: W/O droplets produced in the first flow-focusing region (panel a) are incorporated into a second aqueous continuous phase to produce the W/O/W structure. (d) Fluorescence micrograph of W/O/W emulsions produced, as described in the main text, and collected on a glass slide. The middle (decane) phase fluoresces as a result of Nile red dye used in the oil phase during formation.

between the core and continuous phase. The concomitant adsorption of silica and Nile red is therefore restricted to the two interfaces. As hypothesized by Poortinga,³ the oil layer is replaced by ambient air at the completion of the freeze-drying process.

3.2. Reconstitution. Antibubbles are created by reconstituting the freeze-dried product in DI water at a typical concentration of 1–2 wt %. Upon reconstitution, the air shell is preserved by the dense layer of hydrophobic silica at the outer air–water interface. The desiccated core is quickly rehydrated through the absorption of water vapor from the dissolved continuous phase, and the antibubble is thus produced.⁴ A CSLM micrograph of an antibubble formed after reconstitution of the freeze-dried double emulsion in water is shown in Figure 3. The use of the fluorescent dye Nile red in the oil phase at the time of initial (W/O/W) template formation allows for the positive identification of the once decane, now air layer. We expect that, during the removal of the oil phase, Nile red adsorbs onto the hydrophobic surface of the silica particles, as has been shown for other hydrophobic dyes.¹⁴ The Nile red signal in Figure 3 thus indicates the presence of a rather thick layer of aggregated silica particles at the interfaces.

When the double emulsion (W/O/W) templates were compared to the reconstituted freeze-dried emulsion (antibubbles), an increase in the average size, in terms of both core diameter and total combined core–shell diameter, was observed (Figure 4). We expect that the increase in core size may be the result of a difference in osmotic pressure between the core of the double emulsion and the outer water phase of the reconstituted antibubble suspension, which leads to the uptake of water vapor by the core. The increase in the total core–shell diameter might be explained as follows. Freeze-dried material inherently contains micropores. Upon reconstitution, these micropores will initially form microbubbles. As these microbubbles are not stabilized, Ostwald ripening will make the (much larger) antibubbles grow at the expense of the microbubbles. The fact that the slight growth of the antibubbles does not lead to any observable destabilization could be because the concentration of silica particles used in our study is sufficiently high to form a multilayer network of adsorbed particles that can still stabilize the interfaces after some expansion.¹⁴

Whether the structures produced by reconstitution of the freeze-dried double emulsions are truly antibubbles depends on

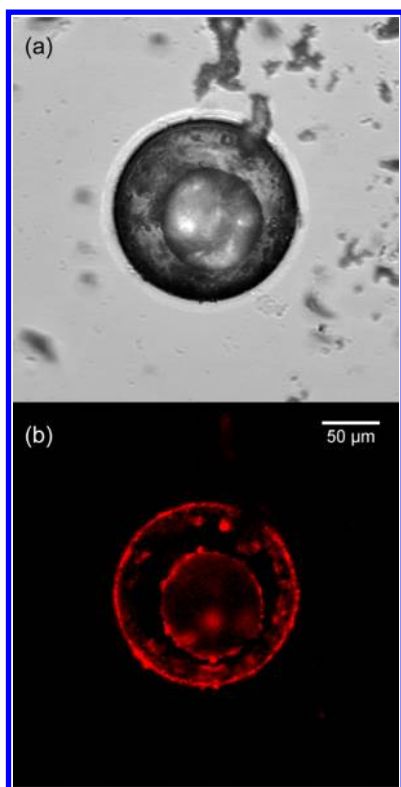


Figure 3. CLSM micrographs of an antibubble produced after redispersion of freeze-dried W/O/W emulsions in DI water. (a) Bright-field and (b) fluorescence images showing the presence of Nile red, localized at the core and continuous phase boundaries, which suggests the replacement of oil with air as the middle (shell) region.

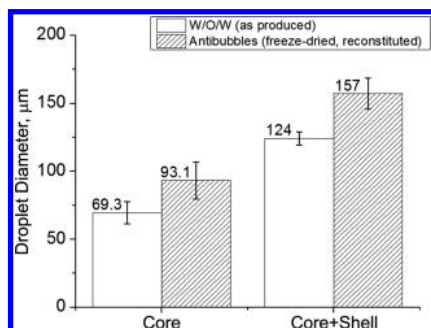


Figure 4. Average size of emulsion droplets (between W/O/W, as produced) and antibubbles (after freeze-drying and redispersion in water) with regard to the evolution of both core and oil phases. Droplet diameter was measured by use of image analysis software (ImageJ, National Institutes of Health, Bethesda, MD). Error bars indicate coefficient of variation.

whether a shell of gas (air) exists between the two aqueous phases.¹⁵ The interpretation of a hollow shell, however, is neither trivial nor as easily identifiable as it is in similar structures of different constructions (e.g., gas-filled micro-particles).^{16,17} Accordingly, the existence of the air layer is deduced in the following manner. First, the presence of the fluorescent probe Nile red at the two interfaces, and not dispersed within the phase itself, suggests a middle region that is no longer oil (decane). Second, when the material is reconstituted in 0.5 wt % Tween 80, we observe a rapid collapse of the structures (Figure 5). It has previously been shown that surfactants can displace adsorbed particles from the

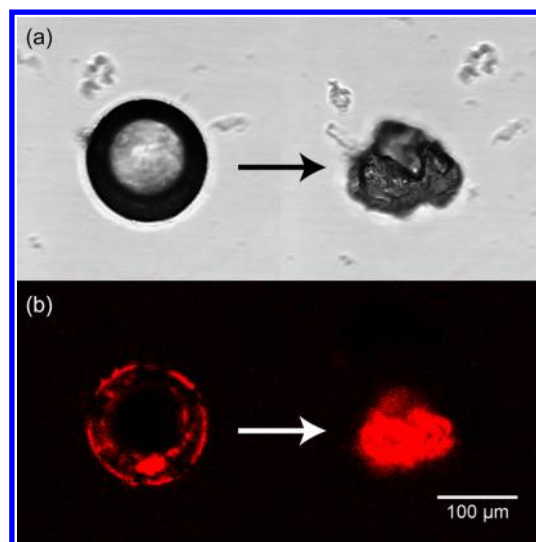


Figure 5. CLSM micrograph of an antibubble, before (left) and after (right) collapse when redispersed in 0.5 wt % Tween 80. (a) Bright-field and (b) fluorescence images showing how the once intact air shell (left) is evacuated upon destabilization and quickly compresses upon release of the inner aqueous phase. Contact between the two aqueous phases results in a rapid coalescence of the core with the surrounding solution. The time for collapse, between intact (left) and completely collapsed (right), occurs between two consecutive frames and so can be estimated by the frame rate to be ≤ 109 ms.

interface of bubbles, leading to their destabilization.¹⁸ Antibubbles stabilized by surfactants are known to be highly unstable,¹ and thus the addition of surfactant will lead to a prompt coalescence of the inner droplet with the outer aqueous phase. As a result, the surrounding air phase instantaneously shrinks to a fraction of its original volume, leaving the remnants of crumpled shells behind, the crumpled shell being a signature of a particle-stabilized interface.¹⁹ The fact that the core mixes instantaneously with the surrounding aqueous phase strongly suggests that the core is aqueous too. We thus conclude that our structures are indeed antibubbles.

The successful conversion of double emulsion droplets into antibubbles through the removal of a volatile oil by freeze-drying followed by reconstitution is not straightforward. Wang et al.²⁰ used freeze-drying to remove a volatile oil from a phospholipid-stabilized double emulsion but obtained liposomes instead of antibubbles. We hypothesize that the use of Pickering stabilization and a solute, in this case maltodextrin, that forms a sufficiently strong glass during freeze-drying is crucial to the production of antibubbles.

3.3. Characterization. We did not explicitly study the stability of our antibubbles but generally find them to have a lifetime of at least 30 min in water. Antibubble stability is primarily attributed to the steric hindrance conferred by a rigid shell of strongly adsorbed colloidal silica at each interface. Steric stabilization is further enhanced by the polymer-induced (partial) flocculation of silica.¹¹ As has been characterized for many Pickering-stabilized systems,^{5,6} the high energy of adsorption required to remove such particles from the interface, along with the strength of particle aggregation, thus prevents their displacement from the shell. PVA is also implicated in the inhibition of ice nucleation during freeze-drying, which suggests a secondary role to maltodextrin in cryoprotection of the double emulsion templates.²¹

We consider the influence of oil layer thickness on the production of antibubbles. More specifically, we find that for the successful conversion of W/O/W templates into antibubbles, the oil layer must constitute some minimally sufficient volume fraction with respect to the total droplet volume. We reached this conclusion by modulating the number of dripping (versus jetting) instabilities in the W/O/W formation process to effect double emulsions of significantly thinner shells (refer to Supporting Information). To this end, using the same CFF devices and fluid phases described herein and methods that have been described elsewhere,²² relative flow rates were adjusted so as to effect a dripping instability in the first junction (W/O) that breaks into a thin-shelled W/O/W emulsion by a jetting instability at the second junction.²³ Following the removal of the middle phase solvent by freeze-drying and reconstitution of the resulting powder, a discrete core-shell structure was observed; however, neither phase could be distinguished as hollow by microscopy (refer to Supporting Information). Thus, we could not confirm beyond doubt the formation of antibubbles from thin-shelled W/O/W templates. Using phase-contrast microscopy, we estimate a shell volume fraction of approximately 15% for the freeze-dried and reconstituted thin-shelled material (refer to Supporting Information). In contrast, when a double emulsion of adequate shell thickness is produced, here roughly 80% of the total W/O/W droplet volume, subsequent solvent removal by freeze-drying seems to allow for the hydrophobic silica to adopt a bilayer configuration separated by a distinct layer of air: an antibubble.

4. CONCLUSION

We have shown the successful microfluidic production of monodisperse core-shell double emulsions and their conversion into stable antibubbles through freeze-drying. The core-shell structure is maintained during conversion, whereas the monodispersity decreases slightly, possibly due to the fact that bubbles are more affected by Ostwald ripening than oil droplets. The well-controlled size and shell thickness of the antibubbles will likely make them respond uniformly to possible release triggers as acoustic,²⁴ magnetic,²⁵ and optical fields.²⁶ These implications are particularly salient in drug delivery, where current methods are often limited by a lack of spatial and temporal resolution.

The possibility of controlled release, combined with the observation that antibubbles rapidly and completely release their cores (within 110 ms) in response to a sensitive trigger, makes antibubbles ideal candidates for drug delivery vehicles in controlled release applications. A particularly attractive modality of targeted drug delivery is ultrasound-mediated release, as it can be applied non-invasively and focused site-specifically. However, in order to be echogenic, the drug carrier must also comprise a significant gas component, and thus their designs are almost exclusively limited to gas-filled microbubbles, in which drugs and targeting ligands constitute but a small fraction on the shell surface.²⁷ Considering the importance of encapsulation efficiency on the dose and delivery of these drugs,^{28,29} a more rational design might be realized using antibubbles with a concentrated drug payload (core) encapsulated by an acoustically active gas shell. Furthermore, the dynamic location of the gas component as a hollow shell, when intact, as opposed to a gas core provides significant opportunity for resolving already-released antibubbles from those that may still be active i.e., intact.

■ ASSOCIATED CONTENT

■ Supporting Information

Four movies and five figures with experimental details, production of double emulsions, account of antibubble collapse, additional considerations regarding thin-shelled material, and determinations of emulsion size and distribution. This material is available free of charge via the Internet at <http://pubs.acs.org>

■ AUTHOR INFORMATION

Corresponding Author

*E-mail hastone@princeton.edu.

Notes

The authors declare no competing financial interest.

■ ACKNOWLEDGMENTS

We acknowledge partial funding from the Princeton Center for Complex Materials, a MRSEC supported by NSF Grant DMR 0819860. We thank Professor R. K. Prud'homme for use of the VirTis benchtop freeze-dryer. J.E.S. thanks the Complex Fluids Group for the guidance, training, and mentorship made possible through the Princeton University VSRC program.

■ REFERENCES

- (1) Dorbolo, S.; Reyssat, E.; Vandewalle, N.; Quéré, D. Aging of an antibubble. *EPL* **2005**, *69*, 966.
- (2) Stong, C. L. The amateur scientist: Curious bubbles in which a gas encloses a liquid instead of the other way around. *Sci. Am.* **1974**, *230*, 116–121.
- (3) Poortinga, A. T. Micron-sized antibubbles with tunable stability. *Colloids Surf., A* **2013**, *419*, 15–20.
- (4) Poortinga, A. T. Long-lived antibubbles: Stable antibubbles through Pickering stabilization. *Langmuir* **2011**, *27*, 2138–2141.
- (5) Binks, B. P.; Lumsdon, S. O. Transitional phase inversion of solid-stabilized emulsions using particle mixtures. *Langmuir* **2000**, *16*, 3748–3756.
- (6) Aveyard, R.; Binks, B. P.; Clint, J. H. Emulsions stabilised solely by colloidal particles. *Adv. Colloid Interface Sci.* **2003**, *100–102*, S03–S46.
- (7) Duffy, D. C.; McDonald, J. C.; Schueller, O. J. A.; Whitesides, G. M. Rapid prototyping of microfluidic systems in poly-(dimethylsiloxane). *Anal. Chem.* **1998**, *70*, 4974–4984.
- (8) Schneider, M. H.; Willaime, H.; Tran, Y.; Rezgui, F.; Tabeling, P. Wettability patterning by UV-initiated graft polymerization of poly(acrylic acid) in closed microfluidic systems of complex geometry. *Anal. Chem.* **2010**, *82*, 8848–8855.
- (9) Barthel, H.; Binks, B. P.; Dyab, A.; Fletcher, P. *Multiple emulsions*. Eur. Patent EP1350556, 2003.
- (10) Simovic, S.; Prestidge, C. A. Hydrophilic silica nanoparticles at the PDMS droplet–water interface. *Langmuir* **2003**, *19*, 3785–3792.
- (11) Sander, J. S.; Isa, L.; Rühs, P. A.; Fischer, P.; Studart, A. R. Stabilization mechanism of double emulsions made by microfluidics. *Soft Matter* **2012**, *8*, 11471–11477.
- (12) Subramaniam, A. B.; Abkarian, M.; Stone, H. A. Controlled assembly of jammed colloidal shells on fluid droplets. *Nat. Mater.* **2005**, *4*, 553–556.
- (13) Oetjen, G. W.; Haseley, P. *Freeze-Drying*, 2nd ed.; Wiley-VCH: Weinheim, Germany, 2004.
- (14) Juárez, J. A.; Whitby, C. P. Oil-in-water Pickering emulsion destabilisation at low particle concentrations. *J. Colloid Interface Sci.* **2012**, *368*, 319–325.
- (15) Dorbolo, S.; Caps, H.; Vandewalle, N. Fluid instabilities in the birth and death of antibubbles. *New J. Phys.* **2003**, *5*, 161.
- (16) Duncanson, W. J.; Abbaspourad, A.; Shum, H. C.; Kim, S. H.; Adams, L. L. A.; Weitz, D. A. Monodisperse gas-filled microparticles from reactions in double emulsions. *Langmuir* **2012**, *28*, 6742–6745.

- (17) Chen, H.; Li, J.; Wan, J.; Weitz, D. A.; Stone, H. A. Gas-core triple emulsions for ultrasound triggered release. *Soft Matter* **2012**, *9*, 38–42.
- (18) Subramaniam, A. B.; Abkarian, M.; Mahadevan, L.; Stone, H. A. Mechanics of interfacial composite materials. *Langmuir* **2006**, *22*, 10204–10208.
- (19) Kim, P.; Abkarian, M.; Stone, H. A. Hierarchical folding of elastic membranes under biaxial compressive stress. *Nat. Mater.* **2011**, *10*, 952–957.
- (20) Wang, T.; Deng, Y.; Geng, Y.; Gao, Z.; Zou, J.; Wang, Z. Preparation of submicron unilamellar liposomes by freeze-drying double emulsions. *Biochim. Biophys. Acta: Biomembr.* **2006**, *1758*, 222–231.
- (21) Wowk, B.; Leitl, E.; Rasch, C. M.; Mesbah-Karimi, N.; Harris, S. B.; Fahy, G. M. Vitrification enhancement by synthetic ice blocking agents. *Cryobiology* **2000**, *40*, 228–236.
- (22) Seo, M.; Paquet, C.; Nie, Z.; Xu, S.; Kumacheva, E. Microfluidic consecutive flow-focusing droplet generators. *Soft Matter* **2007**, *3*, 986–992.
- (23) Abate, A. R.; Thiele, J.; Weitz, D. A. One-step formation of multiple emulsions in microfluidics. *Lab Chip* **2011**, *11*, 253–258.
- (24) Postema, M. *Fundamentals of Medical Ultrasonics*; Spon Press: New York, 2011.
- (25) Silpe, J. E.; McGrail, D. W. Magnetic antibubbles: Formation and control of magnetic macroemulsions for fluid transport applications. *J. Appl. Phys.* **2013**, *113*, No. 17B304.
- (26) Wu, G.; Mikhailovsky, A.; Khant, H. A.; Fu, C.; Chiu, W.; Zasadzinski, J. A. Remotely triggered liposome release by near-infrared light absorption via hollow gold nanoshells. *J. Am. Chem. Soc.* **2008**, *130*, 8175–8177.
- (27) Klibanov, A. L. Targeted delivery of gas-filled microspheres, contrast agents for ultrasound imaging. *Adv. Drug Delivery Rev.* **1999**, *37*, 139–157.
- (28) Soppimath, K. S.; Aminabhavi, T. M.; Kulkarni, A. R.; Rudzinski, W. E. Biodegradable polymeric nanoparticles as drug delivery devices. *J. Controlled Release* **2001**, *70*, 1–20.
- (29) Hamblett, K. J.; Senter, P. D.; Chace, D. F.; Sun, M. M. C.; Lenox, J.; Cervený, C. G.; Kissler, K. M.; Bernhardt, S. X.; Kopcha, A. K.; Zabinski, R. F.; Meyer, D. L.; Francisco, J. A. Effects of drug loading on the antitumor activity of a monoclonal antibody drug conjugate. *Clin. Cancer Res.* **2004**, *10*, 7063–7070.